Celal Bayar University Journal of Science

Comparative Performance Analysis of Surface Mounted Permanent Magnet Synchronous Generators

Tuğberk Özmen[1]* (ID), Nevzat Onat[2] (ID)

[1] Vocational School of Manisa Technical Sciences, 45140, Manisa-Turkey
[2] Department of Electrical and Electronics Engineering, Manisa Celal Bayar University, 45140, Manisa-Turkey
* tugberk.ozmen@cbu.edu.tr
*Orcid: 0000-0002-8636-6091

Abstract

One of the generator types used in generation electrical energy is permanent magnet synchronous generator (PMSG). In this study, a surface mounted permanent magnet synchronous machine with a 1.5 kW inner rotor was used as a reference generator. The finite element analysis of this generator was conducted via commercial finite element analysis (FEA) software. As a result, phase current and voltages waveforms were measured at a rated load. The characteristics of the PMSG under loaded and unloaded working conditions were examined through the measurements on the experimental setup designed in Electrical Machines Laboratory at the Faculty of Engineering of Manisa Celal Bayar University. The values obtained from the open-circuit tests were compared with the simulation and manufacturer's catalog data. This paper also contrasted line voltages measured and simulated at 450 rpm as rated speed.

Keywords: Finite elements method, PMSG, surface mounted PMSG.

1. Introduction

Permanent magnet synchronous machines (PMSM) that contain magnets in the rotor are smaller in volume, lighter in weight and have less copper losses, higher power density, and higher efficiency compared to conventional electrical machines [1,2]. Permanent magnet synchronous machines are used as both a motor and a generator in areas such as automotive, space technologies, computer hardware, medical electronics, military applications, robotics, and wind energy systems. Permanent magnet synchronous generators are one of the generator types utilized in converting mechanical energy into electrical energy in wind energy systems.

Electromagnetic analysis of direct-drive permanent magnet synchronous generators can be conducted via finite element method (FEM) and their design can be improved [1, 3, 4]. The auxiliary tooth structure indicated for the stator structure of PMSGs can reduce short circuit current, cogging torque, and torque ripple [5]. Additionally, the computational and experimental performance findings of PMSG can be compared [6]. Design improvements were made to increase the torque capacity of PMSG and close values were obtained as a result of comparison between FEM and analytical

results [7-10]. The effects of magnet type on PMSG performance were examined in [11-13]. Measurements were made on the experimental setup and the design parameters were compared for the cases in which different magnets were used [11]. Since the amount of magnet to be used in PMSG is an important factor on the cost of the machine, design studies were carried out to reduce the amount of magnet used in the rotor and improve the output power [14-17]. PMSGs are classified as radial or axial depending on the path followed by the magnetic flux. In the hybrid design where radial and axial parts are used together, the power density value is increased 9.4 times [18]. The performance of PMSGs can also be examined over the number of phases. The output parameters of the PMSG designed as five phases were compared by using analytical calculation, FEM, and experimental measurement results. In addition, the study indicated that torque ripples decreases if a PMSG is designed as a five-phase process [19, 20]. And experimental setups and performance tests required for real-time measurements of PMSGs were provided in the study [21- 23]. A short-circuit fault is a serious safety threat to generators. In terms of reliability, the short-circuit current should be limited to a certain range [24-26]. In order for the generators to be more resistant to failure, studies have been carried out on the winding structure

[27-29]. Cooling methods are also important in terms of design for the effective and safe operation of magnets [30].

In this study, magnetic and electrical analyzes of the PMSG used as a reference were conducted through commercial FEA software. The real-time performance of the generator driven by an induction motor was measured designing an experimental setup. No-load and loaded measurements were made for the reference generator and the induction motor which is rotated by AC motor driver at variable speed. For transient measurements of the generator, National Instrument (NI) data collecting modules and LabVIEW™ software were employed.

The following is a summary of how this paper is organized. Nameplate of the reference generator, values of the design parameters, magnetic and electrical results of the finite element analysis are presented in Section 2 and 3. Section 4 describes the experimental set-up along with the results. Section 5 reviews the comparisons between the nameplate values and the results obtained by the finite element approach and experiments. Discussion and the concluding points are summarized in Section 6 and Section 7.

2. Reference Permanent Magnet Synchronous Generator

A radial flux surface mounted PMSG with an inner rotor is utilized in this study. Table 1 lists the reference generator's catalog information while Table 2 provides the values related to the design parameters. The model of the reference generator is shown in Figure 1.

Table 1. Nameplate values of the reference generator.

Parameters	Values
Rated output power	1500 W
Rated rotational speed	450 rpm
Required torque at rated power	35 Nm
Magnet material	NdFeB
Starting torque	< 0.7 Nm
Weight	16.9 kg
Rotor inertia	0.011 kgm
Insulation	H class

Table 2. Design specification of reference generator.

Parameters	Values
Number of slot	72
Number of poles	16
Stator outer diameter	221.5 mm
Rotor outer diameter	157.5 mm
Air gap distance	1 mm
Pole arc ratio	% 84.774
Magnet thickness	5.32 mm
Offset distance	0 mm

3. Finite Element Analysis of the Reference Generator

The finite element method is a useful, low-cost and numerical method that can be used in the analysis of electrical machines based on the solution of differential equations [31]. In order for the method to give more accurate results, it is important that the machine parts are meshed in an appropriate number and the time step is selected with the appropriate value [32]. PMSG was analyzed with FEA software based on finite element method which were created approximately 250000 finite elements mesh and the time step is chosen 0.5 ms. The graph of the phase currents and voltages of PMSG obtained from the two-dimensional analysis of FEA software are respectively presented in Figures 2 and 3. As a result of the analysis, the phase current and voltage of PMSG were obtained as 14.5 A and 37.7 V at a rated load. These values correspond to an active power value of approximately 500 W per phase at a power factor of 0.9.

(a)

(b)

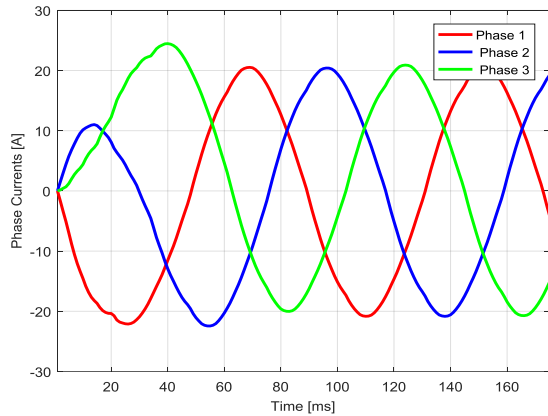**Figure 1.** (a) Stator and (b) rotor of the reference generator.

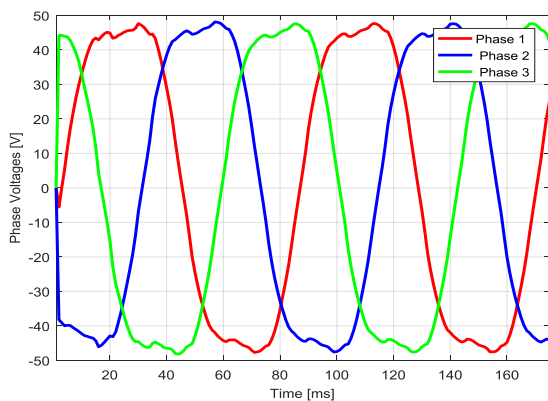**Figure 2.** Phase current waveform at rated load

Figure 3. Phase voltages waveform at rated load

The magnetic flux density distributions of PMSG operating at no-load and rated load are provided respectively in Figures 4 and 5. According to the results of the no-load operating condition, the magnetic flux density in the stator yoke is about 1.2 T, 1.4 T in the stator teeth and 0.7 T in the rotor yoke. According to the results of full-load operating condition, the magnetic flux density in the stator yoke is approximately 1.25 T, 1.5 T in the stator teeth, and around 1 T in the rotor yoke.

4. Experimental Results

An experimental set-up was developed in the Electrical Machines Laboratory at the Faculty of Engineering of Manisa Celal Bayar University to measure the PMSG, which was utilized as a reference. The paper focuses on the characteristics of the PMSG under loaded and unloaded working conditions by examining the measurements. Figure-6 shows the experimental set-up of the reference PMSG consisting of an AC motor driver, an induction motor with 4 poles and 1.1 kW power, a load, energy analyzers, and an oscilloscope.

Cogging torque, induced voltage, THD and core losses can be examined with the no-load operation tests. The measurements made under the no-load operating conditions of the PMSG revealed that there are different

induced voltages at variable speed in the stator windings. Since there is no current in the stator windings in this experiment, the open circuit voltage depends only on the rotation speed. Open circuit voltage values of the PMSG were obtained between 45V and 75V at speed which are between 300 rpm and 750 rpm. Figure 7 displays the result graphic of the no-load test and this graph shows the operational mode of the generator in case of a possible failure.

Due to the reverse magnetic field occurring in the short circuit fault in the PMSG stator windings, demagnetization may occur on the magnets and this can be damage to the machine. In the short circuit experiment, the current values depending on the speed were measured as shown in Figure-8. In the experiment, the highest short circuit current was approximately 5.5 A at 31 rpm. The saturation level of the machine can be determined with the graph obtained from the short circuit test.
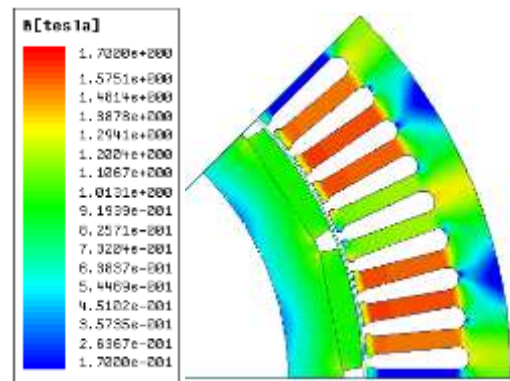

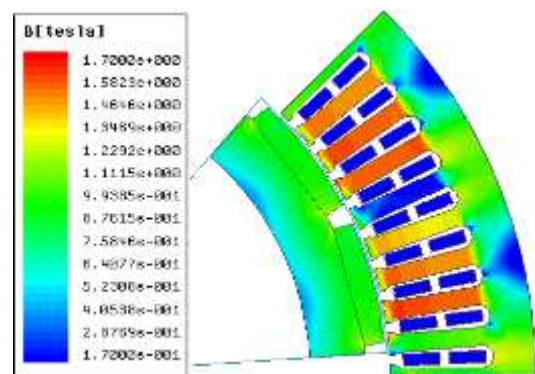**Figure 4.** Magnetic flux density distribution at no load condition

Figure 5. Magnetic flux density distribution at rated load condition

During the load operation tests, current, voltage and speed parameters were analyzed while the load values were taken into account. Figure 9 provides the voltage graph indicating the currents at different speeds. Due to the experimental setup, it is seen that the V-I characteristic behaves as a constant voltage-current

since the generator cannot be loaded sufficiently. The data obtained from this test are used for system design with voltage control in small power wind turbine systems with direct battery connection.

The line voltage graph depending on the speed at different ohmic loads can be seen in Figure 10. This graph indicates that for the same loading condition, the value of the line voltage increases as the speed increases.

The change in generator output current and speed under constant load was also investigated in the experiment. As seen in Figure 11, the change is linear. The slope of the line, on the other hand, increases as the amount of steady load increases. In small power wind turbine applications connected to the battery system through the rectifier, the input current must be within a certain range in order to extend the life of the battery which charged with a constant voltage. By using the data of the speed-current test, this current value can be commented on.
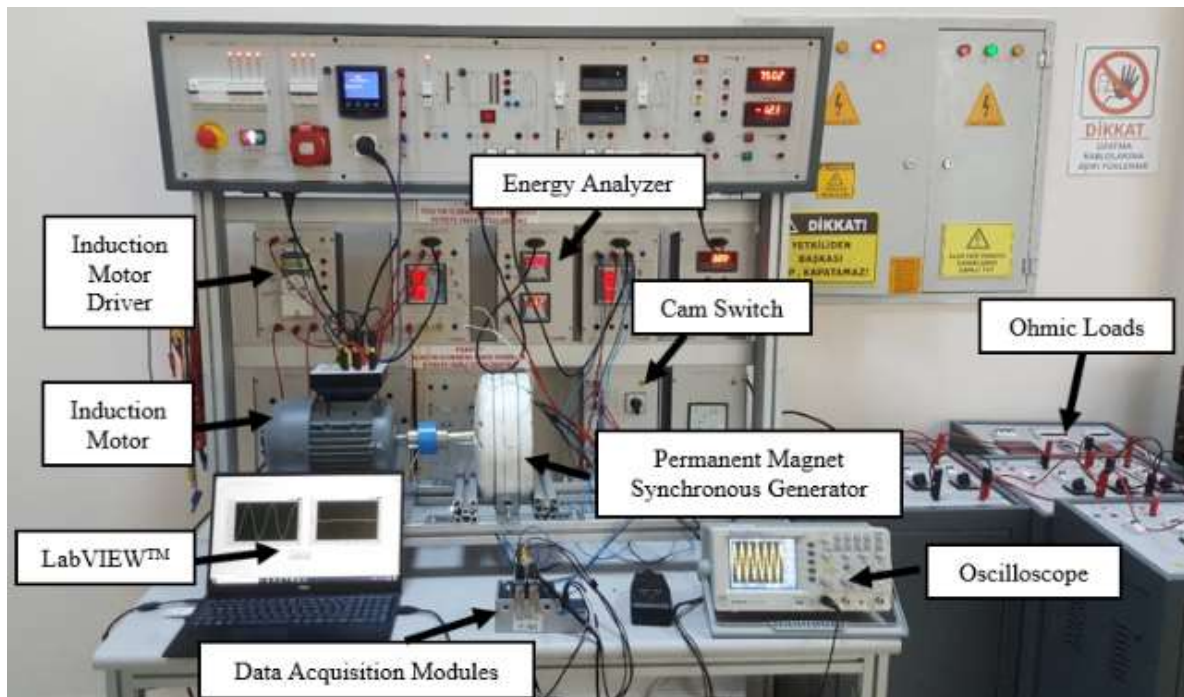

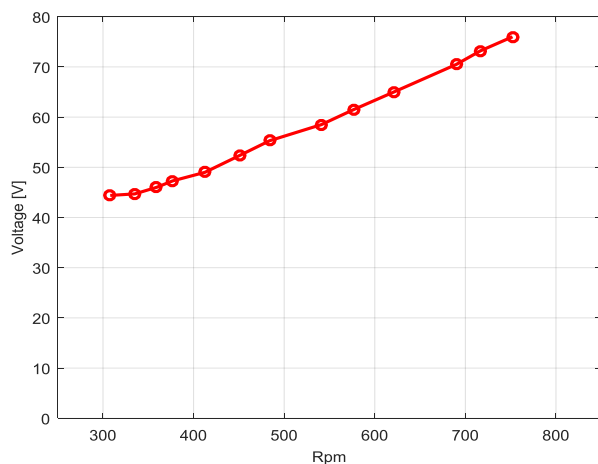
Figure 6. Experimental set-up

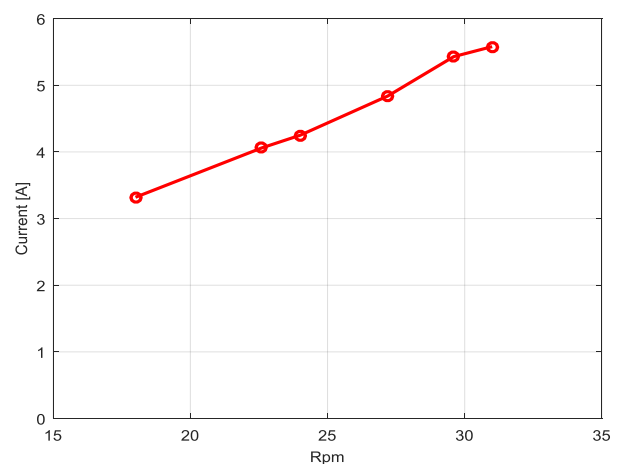**Figure 7.** Experimental results of the induced voltage at no load condition.

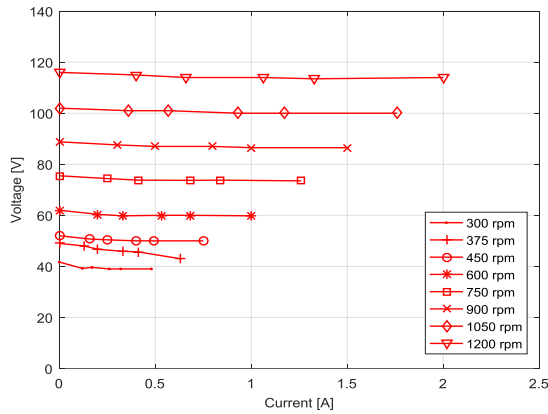**Figure 8.** Short circuit experimental results.

T.Özmen

Figure 9. Voltage graph depending on the load current at different speed.
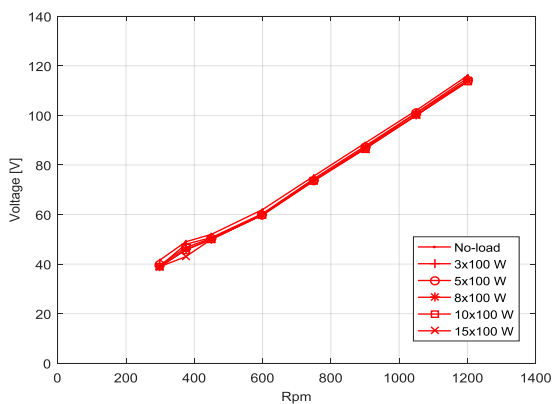

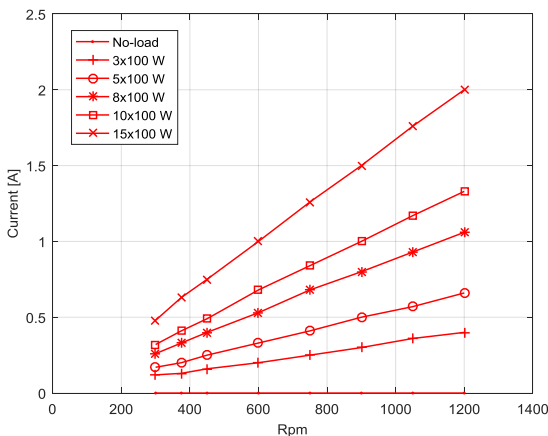**Figure 10.** Voltage graph depending on the speed at different loads.

Figure 11. Load current graph depending on the speed at different loads.

In this study, a conductor and a coil are placed to the winding structure of the reference generator for measurement purposes. The graph of the induced voltage in a conductor and a coil in the no-load operation test is given in Figure 12. These data can be used to test the reliability of the results obtained from software using the finite element method. The value obtained in the experiments was measured about 10 percent lower than the value obtained in the software.
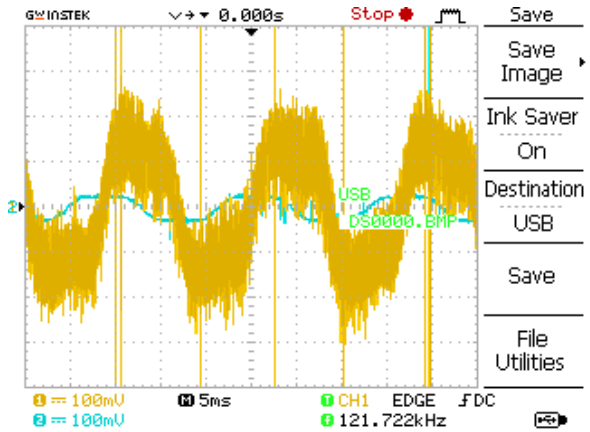

Figure 12. The induced voltage in a conductor and coil.

The experiment setup in Figure 6 was also used for the sudden load operation. Data acquisition modules of National Instruments (NI) company were utilized for measurements, as previously reported. Voltage and current signals were measured with NI 9242 and NI 9246 modules, respectively. These signals were transferred to the computer through LabVIEW^{TM} software.

Figure 13 lists the curves of the current signals related to the sudden load operation performed with the reference PMSG rotating at 450 rpm while the curves related to the voltage signals is provided in Figure 14. When all load groups were turned on at the 77th millisecond of the experiment, the current values rapidly increased, while the voltage value decreased. As can be observed, the voltage dropped by roughly 4.11 percent when the load was activated. According to this result, it is seen that the reliability coefficient of the generator is high in sudden load changes.
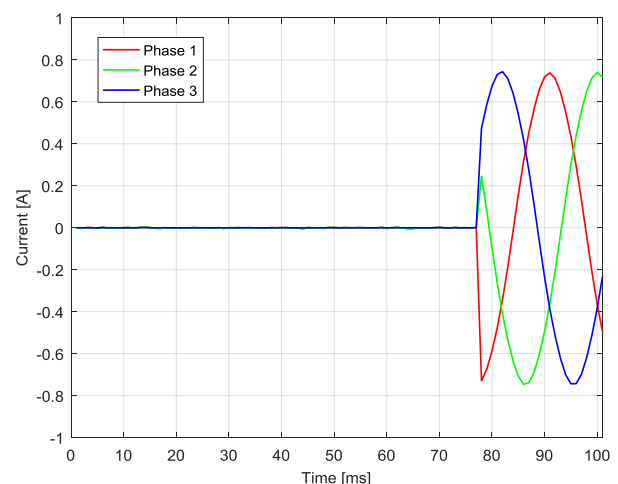

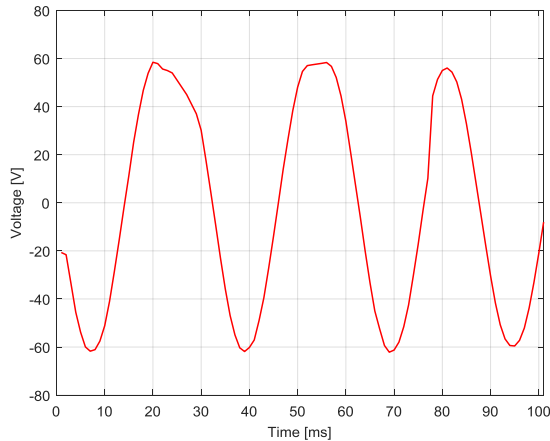**Figure 13.** The sudden load operation current waveform
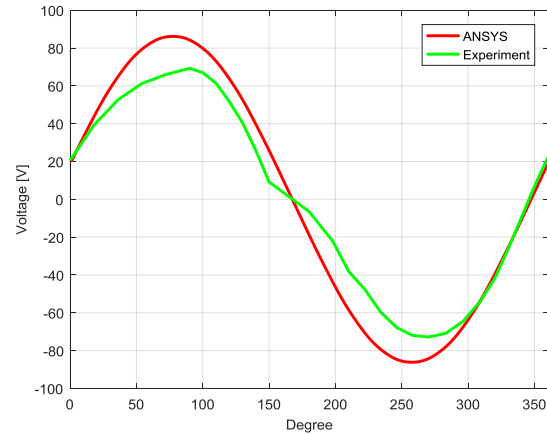
Figure 14. The sudden load operation voltage waveform

5. Comparison Between FEA, Nameplate and Experiments

The comparison of open circuit values which were obtained from the manufacturer's catalog of the reference generator, from experiments and simulations is shown in Figure 15. The difference between curves is most likely due to the difference in magnet strength of the real and simulated generators.

In Figure 16, the line voltage curve acquired from the measurements conducted in the PMSG rotated at 450 rpm in no-load operating conditions was compared to the curve obtained from simulation results. As can be seen in Figure 16, there is a difference of approximately 17.7% in the maximum values of the voltage between the simulation and test results. It is seen that the experimentally obtained values are lower than the data provided by the FEA software under ideal conditions.
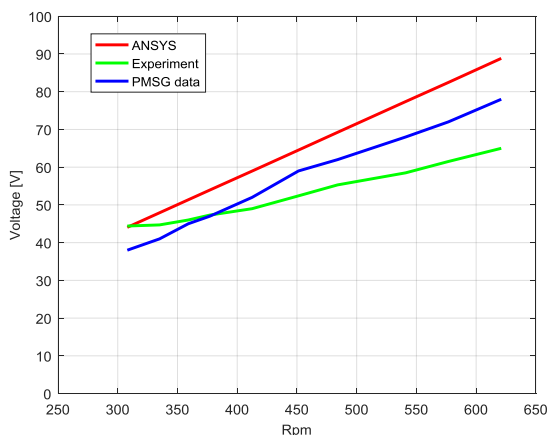

Figure 15. Simulated, experimental and catalog waveform of no-load phase voltage.

Figure 16. Simulated and experimental waveform of no-load phase voltages

6. Discussion

As a result of the finite element analysis of the reference generator conducted via the Maxwell 2D software, phase current at rated load was found as 14.5 A and phase voltage was 37.7 V. In the magnetic analysis carried out through FEA software, it is seen that the magnetic flux density values in different parts of the machine remained within acceptable limits for both no-load and loaded operating conditions. In the no-load experiment which was done for certain speeds between 300 rpm and 750 rpm, the induced voltage in the phase windings was measured between 45 V and 75 V. Current value was measured as 5.5 A at 30 rpm in the short circuit test. The behavior of the reference generator under different load and speed conditions was investigated in the load experiments. The software values achieved under no-load operating conditions are higher than the experiment results and catalog data. The test results were found to be generally lower than the catalog data. The voltage value specified in the catalog for the no-load operation at nominal speed is 9.38% lower than the value obtained in the simulation and 11.19% higher than the value obtained in the experiment.

7. Conclusion

Surface mounted PMSGs provide significant advantages, especially in direct-drive variable-speed turbines (such as wind turbines, mini hydroelectric power plant turbines). With the elimination of the multilayer gearbox, crucial technical benefits such as higher reliability, longer life, lower weight are achieved. They do, however, they also contain important limitations which are electromagnetic, thermal and cooling that limit their development at high power. In this study, the performance of a small powerful generator manufactured for vertical axis wind turbines was analyzed and compared in terms of simulation, experiment, and catalog information. In general, it was

confirmed that actual operating conditions provide lower performance outputs compared to simulation values. The thermal effects generated by the heating of the winding and surface magnets under real operating conditions, as well as extra losses in the mechanical connection, were determined to be the reason of this disparity. According to the results, it can be said that PMSGs produce very stable outputs against sudden load changes and voltage ripples remain at an acceptable level. The specific contribution of this study is to measure the induced voltages in a conductor and coil which placed in the winding structure of an existing PMSG and compare these values with the results obtained in the FEM software. The fact that the values obtained from the software and the values obtained in the experiments were similar, proved the reliability of the analyzes to be made with the software before the PMSGs were produced. The benefits of various control strategies for increasing the output power of the reference generator will be examined in a subsequent study.

Authors' Contributions

Tuğberk ÖZMEN: Drafted and wrote the manuscript, conducted the experiment, and analyzed the results.
Nevzat ONAT: Supervised the experiment's progress, interpretation process of the results and helped preparing the manuscript.

Ethics

There are no ethical issued after the publication of this manuscript.

References

1. Duan, G, Wang, H, Guo, H, Gu, G. 2010. Direct drive permanent magnet wind generator design and electromagnetic field finite element analysis. *IEEE Transactions on Applied Superconductivity;* 20(3): 1883-1887.

2. Zhou, J, Li, S, Li J, Zhang, J. A Combined Control Strategy of Wind Energy Conversion System with Direct-Driven PMSG, 31st Youth Academic Annual Conference of Chinese Association of Automation, Wuhan, China, 2016, pp 369–374.

3. Deng, QL, Huang, SD, Peng, L. 2009. FEM analysis design on low speed direct-driven permanent magnet generator for wind turbine. *Micromotors Servo Technique;* 42: 9–12.

4. Chen, J, Nayar, CV, Xu, L. 2000. Design and finite-element analysis of an outer-rotor permanent-magnet generator for directly coupled wind turbines. *IEEE Transactions on Magnetics;* 36: 3802–3809.

5. He, Y, Zhao, W, Tang, H, Ji, J. 2020. Auxiliary teeth design to reduce short-circuit current in permanent magnet generators. *CES Transactions on Electrical Machines and Systems;* 4(3): 198-205.

6. Chan, TF, Wang, W, Lai, LL. 2010. Permanent-magnet synchronous generator supplying an isolated load. *IEEE Transactions on Magnetics;* 46(8): 3353-3356.

7. Tapia, JA, Pyrhonen, J, Puranen, J, Lindh, P, Nyman, S. 2012. Optimal design of large permanent magnet synchronous generators. *IEEE Transactions on Magnetics;* 49(1): 642-650.

8. Liuzzi, G, Ludici, S, Parasiliti, F, Villani, M. 2003. Multiobjective optimization techniques for the design of induction motors. *IEEE Transactions on Magnetics;* 39(3): 1261–1264.

9. Sudhoff, SD, Cale, J, Cassimere, B, Swinney, M. Genetic Algorithm Based Design of a Permanent Magnet Synchronous Machine, IEEE International Conference on Electric Machines and Drives (IEMDC), San Antonio, TX, 2005, pp 1011–1019.

10. Sadeghi, S, Parsa, L. 2011. Multiobjective design optimization of five-phase halbach array permanent-magnet machine. *IEEE Transactions on Magnetics;* 47(6): pp. 1658–1666.

11. Jang, SM, Seo, HJ, Park, YS, Park, HI, Choi, JY. 2012. Design and electromagnetic field characteristic analysis of 1.5 kW small scale wind power generator for substitution of Nd-Fe-B to ferrite permanent magnet. *IEEE Transactions on Magnetics;* 48(11): 2933-2936.

12. Sun, T, Kwon, SO, Lee, JJ, Hong, JP. Investigation and Comparison of System Efficiency on the PMSM Considering Nd-Fe-B Magnet and Ferrite Magnet, INTELEC 2009-31st International Telecommunications Energy Conference, Incheon, Korea (South), 2009, pp 1–6.

13. Dorrell, DG, Hsieh,, MF, Knight, AM. 2012. Alternative rotor designs for high performance brushless permanent magnet machines for hybrid electric vehicles. *IEEE Transactions on Magnetics;* 48(2): 835–838.

14. Fang, H, Wang, D. 2016. A novel design method of permanent magnet synchronous generator from perspective of permanent magnet material saving. *IEEE Transactions on Energy Conversion;* 32(1): 48-54.

15. Kowal, D, Sergeant, P, Dupre, L, Karmaker, H. 2015. Comparison of frequency and time-domain iron and magnet loss modeling including PWM harmonics in a PMSG for a wind energy application. *IEEE Transactions on Energy Conversion;* 30(2): 476–486.

16. Yamazaki, K, Fukushima, N. 2010. Iron loss model for rotating machines using direct eddy current analysis in electrical steel sheets. *IEEE Transactions Energy Conversion;* 25(3): 633–641.

17. Huang, WY, Bettayeb, A, Kaczmarek, R, Vannier, JC. 2010. Optimization of magnet segmentation for reduction of eddy-current losses in permanent magnet synchronous machine. *IEEE Transactions Energy Conversion;* 25(2): 381–387.

18. Ishikawa, T, Amada, S, Segawa, K, Kurita, N. 2017. Proposal of a radial-and axial-flux permanent-magnet synchronous generator. *IEEE Transactions on Magnetics;* 53(6): 1-4.

19. Kumar, RR, Singh, SK, Srivastava, RK, Saket, RK. 2020. Dynamic reluctance air gap modeling and experimental evaluation of electromagnetic characteristics of five-phase permanent magnet synchronous generator for wind power application. *Ain Shams Engineering Journal;* 11(2): 377-387.

20. Kumar, RR, Singh, SK, Srivastava RK. Thermal Modelling of Dual Stator Five-Phase Permanent Magnet Synchronous Generator, IEEE Transportation Electrification Conference (ITEC-India), Pune, India, 2017, pp 1–6.

21. Cano, L, Arribas, L, Cruz, I. 2004. 1.5 kW permanent magnets synchronous generator experimental bench test. *Department of Renewable Energie, CIEMAT.*

22. Advanced Energy, Permanent magnet generator performance testing, Report, January 23, 2014.

23. Standard IEC 60034-4. Rotating Electrical Machines. Part 4: Methods for Determining Synchronous Machine Quantities from Tests. Jun 1997

24. Zhao, W, Xu, L, Liu, G. 2018. Overview of permanent-magnet fault-tolerant machines: Topology and design. *CES Transactions on Electrical Machines and Systems*; 2(1): 51-64.

25. Wang, S, Sun, Y, Huang, Z, Mu, S. 2018. Analysis of stator internal phase-to-phase short circuit in the 12-phase synchronous generator with rectifier-load system. *IEEE Transactions on Energy Conversion*; 33(1): 299-311.

26. Song, X, Wang, Y, Liu, D, Wang, S, Liang, D. 2019. Short-circuit characteristics of a high temperature superconducting wind turbine generator employing a segmented armature winding. *IEEE Transactions on Applied Superconductivity;* 29(5): 1-5.

27. Afinowi, IAA, Zhu, ZQ, Guan, Y, Mipo, JC, Farah, P. 2016. Electromagnetic performance of stator slot permanent magnet machines with/without stator tooth-tips and having single/double layer windings. *IEEE Transactions on Magnetics*; 52(6): 1-10.

28. Choi, G, Jahns, TM. 2016. Reduction of eddy current losses in fractional-slot concentrated-winding synchronous PM machines. *IEEE Transactions on Magnetics*; 52(7): 1-4.

29. Li, D, Zou, T, Qu, R, Jiang, D. 2018. Analysis of fractional-slot concentrated winding PM vernier machines with regular open-slot stators. *IEEE Transactions on Industry Applications*; 54(2): 1320-1330.

30. Tong, W, Wu, S, An, Z, Zhang, H, Tang, R. Cooling System Design and Thermal Analysis of Multibrid Permanent Magnet Wind Generator, 2010 International Conference on Electrical and Control Engineering, Wuhan, China, 2010, pp 3499–3502.

31. Gulbahce, MO, Kocabas, DA, Nayman, F. Investigation of The Effect of Pole Shape on Braking Torque for a Low Power Eddy Current Brake by Finite Elements Method, 2013 8th International Conference on Electrical and Electronics Engineering (ELECO), Bursa, Turkey, 2013, pp 263-267.

32. Gulbahce, MO, Kocabas, DA, Habir, I. Finite Elements Analysis of a Small Power Eddy Current Brake, proceedings of 15th International Conference MECHATRONIKA, Prague, Czech Republic, 2012.